Thermochimica Acta, 238 (1994) 371–395
Elsevier Science B.V., Amsterdam
SSDI 0040-6031(93)01581-M

Selected thermodynamic aspects of the influence of pressure on polymer systems

Servaas Vleeshouwers * and Erik Nies

Department of Polymer Technology, Eindhoven University, P.O. Box 513, 5600 MB Eindhoven (The Netherlands)

(Received 19 May 1993; accepted 25 October 1993)

Abstract

The influence of pressure and temperature on a selection of physical/thermodynamic properties is explored. In the first part, some experimental facts of the thermal behaviour are summarized. The equations of state of melts and glassy amorphous polymers are considered. From this, the pressure dependence of the glass transition temperature is derived.

As a first illustration of the non-equilibrium nature of the glassy state, the impact of cooling rate on the glass transition temperature is demonstrated. In a further demonstration of the non-equilibrium character, the inevitable physical ageing is illustrated for simple and combined temperature and pressure jump experiments. Finally, some examples of thermodynamic properties at high frequencies, such as the dynamic compressibility, are discussed.

In the second part of this contribution, a model of the dense disordered state, pertinent to chain and small molecule fluids, is discussed. The model is based on a cell model with additional configurational disorder provided by vacancies. In the theory, two parameters define the intermolecular interactions. In polyatomic systems, a third parameter is introduced, quantifying molecular modes of motion which are perturbed by the surroundings. The theory is successfully applied to describe the equation-of-state behaviour of pure constituents. Typically, the experimental data are described within the experimental uncertainty of the measuring technique.

In order to facilitate a discussion of the non-equilibrium and high-frequency properties, the equilibrium theory is complemented with a stochastic formalism. This combination allows the influence of formation parameters on the glassy state to be discussed. For instance, the dependence of the glass transition temperature on cooling rate and pressure is predicted. Also the equation of state of the resulting glasses is predicted and compares favourably with the experimental data. Finally, this method is also applied to address the frequency dependence of thermodynamic properties in general.

The presented formalism opens the way to discuss the dependence of the ultimate properties of materials, obtained along a processing route, on the non-equilibrium

* Corresponding author.

conditions experienced during processing. In particular, the importance of formation history and physical ageing is clarified.

INTRODUCTION

The tractability of polymers is greatly related to the ease with which polymers can be formed into commercial products by a variety of processing techniques. In most processing conditions, pressure, in combination with temperature, plays a prominent role. For instance, each individual small material element in a polymer melt which is subjected to, for example, an injection moulding process, perceives a complicated formation hisotry during the short process cycle. Important variables defining this formation history are, for example, the temperature and pressure as well as the rates of cooling/heating and pressurizing sensed by the material element. For instance, during injection moulding, cooling rates of $100\,K\,s^{-1}$ and pressurizing rates of $30\,MPa\,s^{-1}$ are not exceptional. Furthermore, if the final product is used in the glassy state, the formation history also influences the ultimate properties of the products. For instance, the dimension stability of precision-formed components are particularly sensitive to the formation history, i.e. the precise course by which this glassy state was accomplished. In the present paper, the influence of pressure and temperature on equilibrium, as well as the time-dependent thermodynamic thermal properties, is addressed. In the first part, experimental details are considered. The equation of state of amorphous polymers in the melt and glassy state is presented. Furthermore, the situations in which the time dependence of the thermodynamic properties become apparent are summarized. The first examples comprise the influence of pressure and cooling rate on the glass transition temperature, the path dependence of the equation of state in the glassy state, and the subsequent volume relaxation behaviour. Finally, the high-frequency analogue of the compressibility and its course with pressure and temperature is illustrated.

The experimental observations are discussed in terms of a theory appropriate to the liquid state. The model rests on a quasi-lattice or cell approximation with additional disorder obtained by allowing for vacant lattice positions defining a structure function h, i.e. the fraction of vacant cells on the lattice. If the equilibrium theory is complemented with a stochastic formalism, the time-dependence of the structure function h can be evaluated. In doing so, the glass transition is considered to be a consequence of a gradual freeze-in of molecular relaxation times large in comparison with observation times. Consider the properties of the polymer glass as a non-equilibrium which is retraceable to the equilibrium

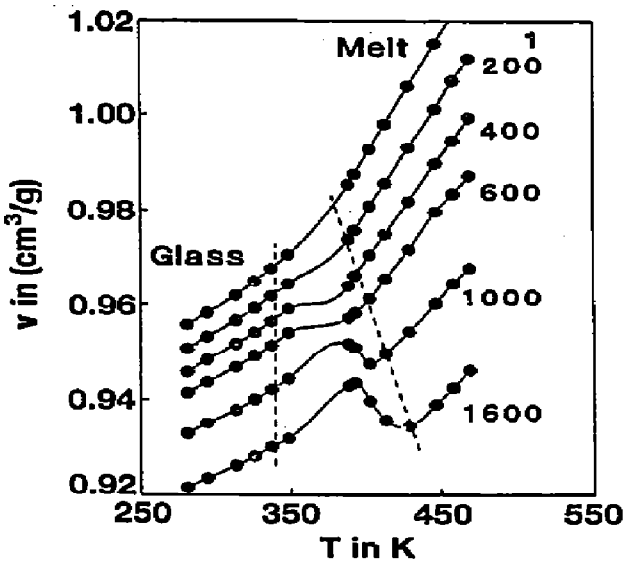

Fig. 1. Equation-of-state data for atactic polystyrene (Dow Stryron 686, $M_n = 90$ kg mol^{-1}, $M_w/M_n = 3$) [2]. Specific volume versus temperature (cooling from the melt at 10 K h^{-1} and subsequently) after isothermal pressurizing at 400 bar h^{-1} from 1 bar to the indicated pressures. The isobars are shown for convenience. The apparatus used is of the bellows type, using mercury as a confining liquid.

PROPERTIES

Equilibrium, glassy state and transition region

A typical example of the equation of state of an amorphous polymer is shwon in Fig. 1. At sufficiently high temperatures, the polymers are in the liquid state and the values of the expansion coefficient $\alpha = (1/v)(\partial v/\partial T)_p$ and compressibility factor $\beta_T = (-1/v)(\partial v/\partial p)_T$ are typical of ordinary liquids. Extensive experimentation on and analysis of polymer melts has taken place [1]. Experimental data collected by Simha and colleagues comprised vinyl-type compounds, whereas Zoller and colleagues also included in their studies various engineering plastics, compatible polymer blends and copolymers.

At sufficiently low temperatures the polymer experiences a transition to the glassy state. The glass transition is typical of amorphous polymers which are unable to crystallize (see Fig. 1) and can be observed in the pvT diagram as a change in slope in the isobars or as a discontinuity in the expansion coefficient and compressibility factor [2]. In the glassy state, values for β_T and α are typical of solids. Several polymers show other transitions in the glassy state [3, 4]. However, often other techniques have to be used to demonstrate their existence.

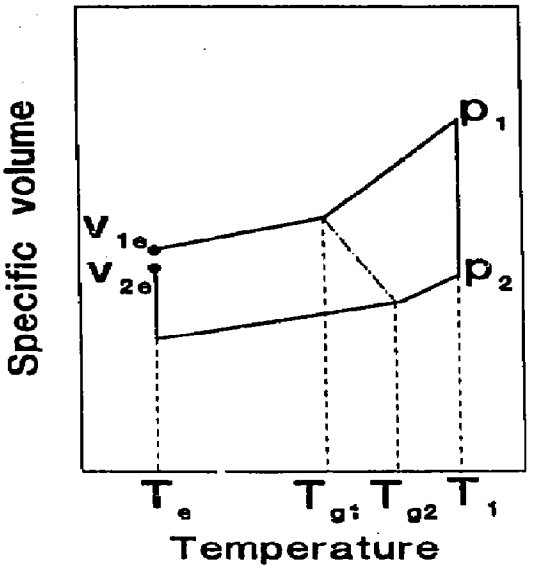

Fig. 2. Schematic volume–temperature diagram for a glass-forming polymer. Two different glass formation routes are shown and discussed in the text.

The study of equilibrium conditions, i.e. in the melt, has the enormous advantage that physical properties have unique values determined by a limited set of microscopic variables. In this case, at a given pressure and temperature, the volume of a single component liquid is uniquely determined by its equation of state. In the glass transition region and the glassy state, this simplicity no longer holds [5, 6]. From the experimental results of, for example, Greiner and Schwarzl [4], McKinney and Goldstein [7] and Kogowski and Filisko [8], it is clearly established that the formation history, i.e. the route of preparation, also influences the equation of state and the other properties of the polymer glass.

Consider as an illustration the situation depicted in Fig. 2. In contrast with polymer liquids, the same limited set of macroscopic variables does not suffice to fix the thermodynamic state of polymer glasses: a polymer melt cooled isobarically at a fixed rate from temperature T_1 at P_1 to a temperature $T_e < T_g$. The polymer glass will be characterized by a volume v_{1e}. The polymer glass at T_1 and P_1 can also be prepared along a different route: first pressurize the melt at T_1 from P_1 to P_2, cool isobarically (at the same fixed rate) to T_e, and finally reduce the pressure to P_1. In this case the volume of the polymer glass will be v_{2e}, i.e. different from v_{1e}. From this example, it is clear that the formation history, i.e. the exact path followed to prepare a particular glassy sample, must be specified and, thus, that the glassy state is not an equilibrium state. In Fig. 2, it can be observed that the value of the glass transition temperature depends on the formation history and, in particular, on pressure.

Experimental details for atactic polystyrene (PS) (Dow Stryron 686,

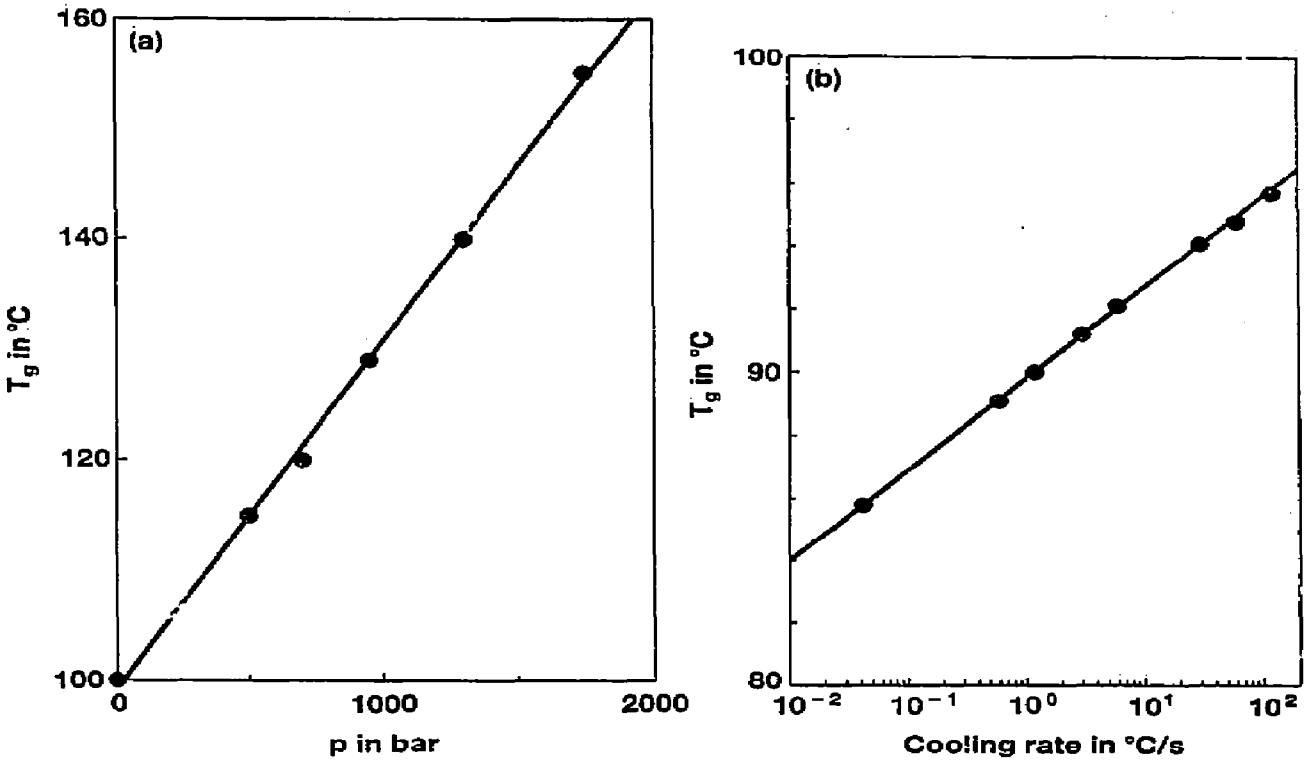

Fig. 3. The variation of the glass transition temperature of atactic polystyrene with (a) pressure [2] during isobaric cooling at 10 K h^{-1} and (b) cooling rate at ambient pressure [4].

$M_n = 90$ kg mol^{-1}, $M_w/M_n = 3$) are shown in Fig. 3(a) [2]. Furthermore, as depicted in Fig. 3(b), the cooling rate also has an influence on the value of the glass transition temperature [4]. This last observation in particular indicates the relevance of kinetic and non-equilibrium conditions for the glass transition.

The onset of the glassy state is, in general, indicated by the sudden change in many properties over a rather narrow region called the glass transition region. The transition can be assigned as the glass transition temperature. One of the most fundamental ways to determine this is by observing the *specific volume*. The T_g can be defined, based on dilatometry experiments, as the temperature of the intercept of the tangents at the glass and melt part of the $v-T$ curve during isobaric cooling or heating. But other properties are also indicative of the glass transition. The *enthalpy* follows the same general trends as the volume in the case of glass formation. Differential scanning calorimetry (DSC) is usually used to measure the derivative of the enthalpy with respect to time, i.e. a heat flow, which at constant heating rate is proportional to the specific heat c_p. With small-angle X-ray scattering (SAXS), neutron scattering and light scattering, *density fluctuations* can be measured. When a polymer is cooled to temperatures below T_g, density fluctuations show a sudden change in

temperature dependence. Also *mechanical properties*, such as the modulus E, the shear creep compliance $J(t)$, the stress relaxation modulus $G(t)$, and the shear viscosity, and their temperature coefficients, change drastically at T_g. The final property with which to study the glass transition is *dielectric relaxation* in which the dielectric permittivity is measured. Usually ε'', the loss part, which exhibits a maximum around T_g, is studied.

Physical ageing

Another aspect of the non-equilibrium conditions becomes apparent in the following experiment: the volume of the polymer glass (prepared by cooling isobarically) as a function of time experiences a continuous densification. This is one aspect of the physical ageing that is typical of glassy systems.

Figure 4 depicts some more detailed experimental results on the volume relaxation behaviour of polyvinylacetate (PVAc) [9]. Polymer samples are jumped (a) from the same initial temperature $T_i = T_g + 5$ K to different final temperatures $T_e < T_i$ with T_e in the neighbourhood of T_g, and (b) from different initial temperatures T_i close to T_g to the same final temperature $T_e = T_g + 5$ K, $T_e > T_i$. The volume relaxation following isothermal pressure jumps is analogous to the temperature jump experiments considered previously. Figure 5 shows the volume relaxation behaviour after jumps from different pressures to atmospheric pressure [10, 11]. All these data can be explained by the free volume concept.

Polymer glasses prepared at atmospheric pressure show physical ageing, i.e. a densification in time. High density glasses can be prepared under high pressure conditions. One can consider then an appropriate formation history so that physical ageing can be reduced or circumvented completely. A tentative scheme for PVAc is the following: the polymer is jumped from the initial temperature $T_i = 313$ K to a temperature T_f (indicated in Fig. 6). The polymer is kept at this temperature until the density is equal to the equilibrium density at another temperature T_f. At this moment the temperature is jumped to this temperature T_i and the volume is monitored with time. Naively, one might hope that no physical ageing will occur because the glass at T_f has attained its equilibrium density. The time response of the glass prepared in this manner is shown in Fig. 6 [9]. It can be observed that the density does not remain constant with time but at first decreases, reaches a minimum, and then returns to the equilibrium density. The polymer appears to possess a memory for its formation history.

A similar effect can be observed with pressure if, for example, the following formation path is followed. The polymer is cooled at high pressure to a temperature T_2. The pressure and temperature are chosen so that the density of the fresh sample is equal to the (equilibrium) density of the sample prepared at atmospheric pressure at T_2. The pressure is then

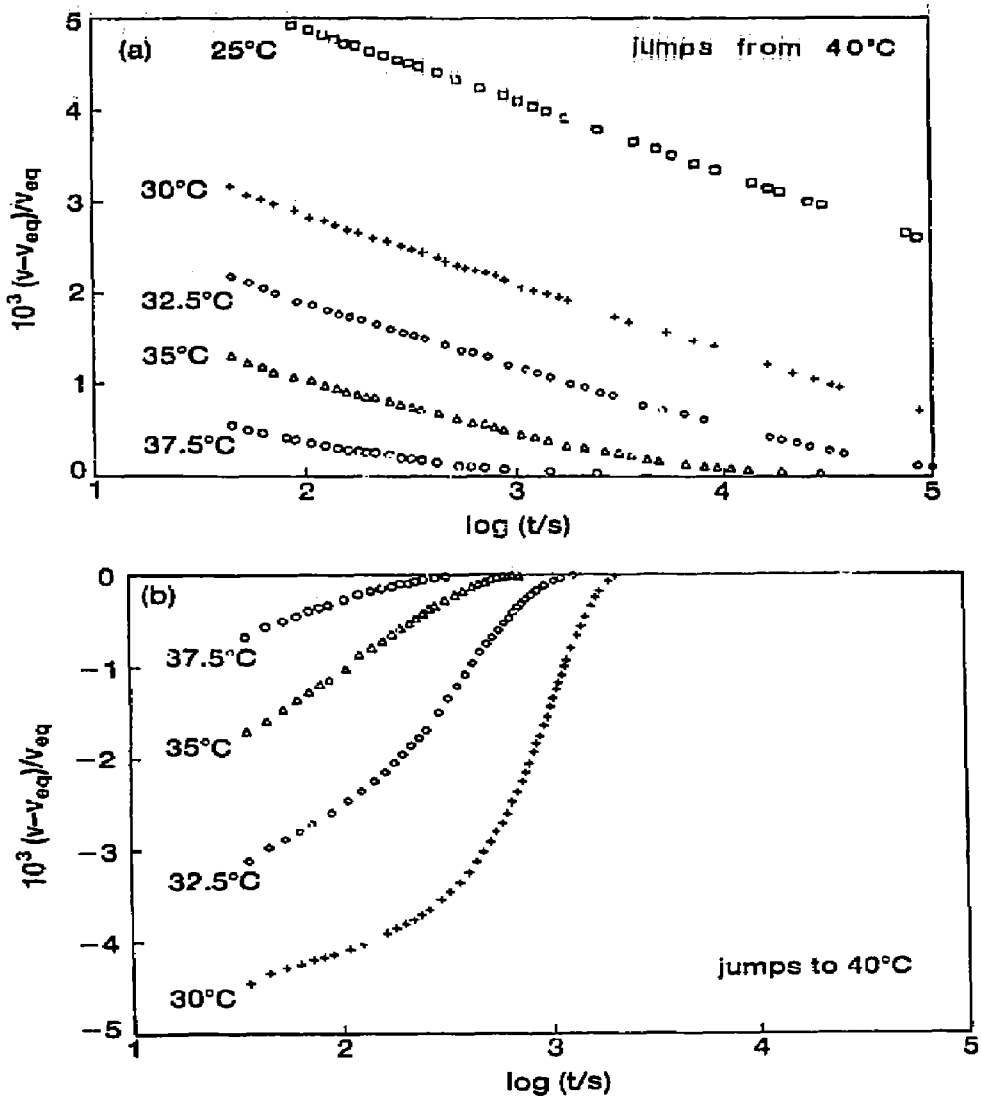

Fig. 4. Volume departure from equilibrium versus time after single temperature jumps for polyvinylacetate with $T_g = 35°C$ measured with a dilatometer [9]. (a) Jumps from 40.0°C to indicated temperatures. (b) Jumps from indicated temperatures to 40.0°C. Thermal equilibrium is reached within 0.02 h.

released and the subsequent time response of the density is followed. A memory effect is also observed in this case. From these experiments, it is clear that the density is not the only factor determining the characteristic behaviour of glasses.

Thermodynamic properties at high frequencies

Although transient and dynamic oscillatory experiments are related to each other by Fourier transforms and thus contain the same time-dependent information, experimentally it is often more convenient to

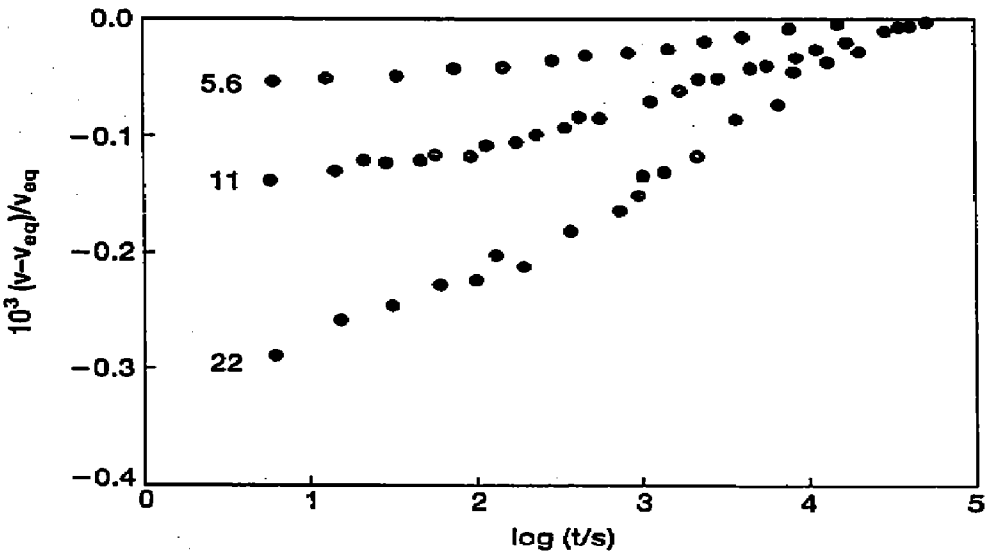

Fig. 5. Volume departure from equilibrium versus time after single pressure jumps from indicated initial pressures (in bar) to atmospheric pressure for atactic polystyrene at 365 K, using a high-pressure dilatometer [10, 11].

perform dynamic oscillatory experiments instead [12]. In these experiments the actual deformations are usually small and at the same time a large constant hydrostatic pressure can be applied. Therefore, these experiments are extremely suitable for studying the influence of pressure on the linear viscoelastic behaviour.

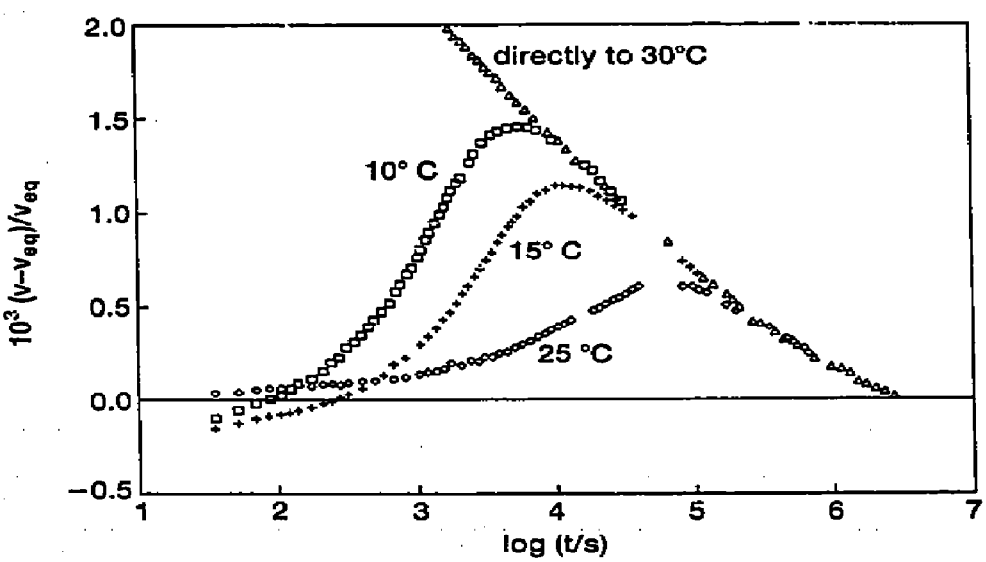

Fig. 6. The effect of combined temperature jumps on the volume relaxation behaviour [9]. The sample is jumped from an initial temperature $T_i = 40°C$ to the indicated temperatures T_1. When the density of the sample is equal to the equilibrium density at temperature $T_f = 30°C$, the sample is jumped to this temperature. The volume relaxation behaviour after this last jump is followed with time.

The most extensive direct measurement of dynamic compression, the frequency analogue of the equilibrium compressibility β_T, has been performed for PVAc in the frequency range 50–1000 Hz and for pressures from 1 to 1000 atm [12].

In analysing these data, the significant pressure and temperature dependence of the limiting bulk compliances at high and low frequencies must be taken into account. From these results, the pressure and temperature dependences at a given frequency can be derived.

In more recent years, a new technique to measure the longitudinal bulk compliance M has become available. Photon correlation spectroscopy presents an elegant, non-destructive technique to measure this quantity as a function of pressure and temperature over a considerable time (or frequency) range [13–15].

EQUILIBRIUM THEORY: HELMHOLTZ FREE ENERGY AND EQUATION OF STATE

The equilibrium theory is based on a quasi-lattice having a fraction of vacant positions, and with the polymer segments sited on the lattice positions. Each unit (segment or molecule) is subjected to thermal motions in the field of its neighbours. This field is computed employing a mean field approximation which places these neighbours onto average positions defined by the sites of the lattice. In order to enhance the configurational disorder, a fraction h of vacant sites is introduced. It may be viewed as an excess free volume function over that prevailing in the fully occupied lattice [16].

The free volume function enters through three factors into the partition function, and hence, also into the Helmholtz free energy A and all the thermodynamic properties derivable from this. These three factors are

(i) A combinatory factor arising from the mixing of empty and occupied sites.
(ii) A free volume term characteristic of cell theories which is computed by approximating the cell potential by a square well.
(iii) A lattice contribution, again characteristic of cell theories.

We note that the resulting expressions for these contributions are functions of the configurational disorder, i.e. the free volume function h. In recent investigations, it has been demonstrated that the external contact fraction q is more appropriate to describe the influence of the configurational disorder [17–21]. This external contact fraction q is related to the free volume function, according to

$$q = \frac{(1-\alpha)y}{(1-\alpha y)} \tag{1}$$

with $\alpha = \gamma(1 - 1/s)$, $\gamma = 2/z$, and $y = (1 - h)$, where z is the lattice

coordination number and s is the number of lattice sites occupied by a molecule of molar mass M.

Introducing c, with $3c$ being the number of external or volume-dependent modes in the s-mer, the abbreviations $a = 1.011$, $b = 1.2045$, the reduced variables $\tilde{p} = p/p^*$, $\tilde{V} = V/V^*$, $\tilde{T} = T/T^*$, and $\eta = 2^{-1/6}y(1-\alpha)/((1-\alpha y)\tilde{\omega}^{1/3})$, with $\tilde{\omega} = y\tilde{V}$, the reduced volume of a lattice site or cell, the Helmholtz free energy A is given by

$$A/NsRT = \frac{\ln(y)}{s} + \frac{(1-y)\ln(1-y)}{y} - \frac{(1-\alpha y)\ln(1-\alpha y)}{\gamma y}$$
$$- \frac{c}{s}\ln(v^*\tilde{\omega}(1-\eta)^3) + \frac{cq}{2s\tilde{T}}(a\tilde{\omega}^{-4} - 2b\tilde{\omega}^{-2}) \quad (2)$$

From the Helmholtz free energy, the pressure equation can be obtained according to

$$p = -\left(\frac{\partial A}{\partial V}\right)_{N,T,y} - \left(\frac{\partial A}{\partial y}\right)_{N,T,V}\left(\frac{\partial y}{\partial V}\right)_{N,T} \quad (3)$$

The temperature and volume or pressure dependence at equilibrium of the characteristic structure function q (or h) is uniquely determined by the minimization of the configurational free energy [16, 17]

$$\left(\frac{\partial A}{\partial y}\right)_{N,T,V} = 0 \quad (4)$$

Performing the necessary algebra, we obtain the two coupled equations [17]

$$\frac{\tilde{p}\tilde{V}}{\tilde{T}} = \frac{1}{(1-\eta)} + \frac{2(1-\alpha)y}{(1-\alpha y)\tilde{T}\tilde{\omega}^2}\left[\frac{a}{\tilde{\omega}^2} - b\right] \quad (5)$$

and

$$1 - \frac{1}{s} + \frac{1}{y}\ln(1-y) - \frac{1}{\gamma y}\ln(1-\alpha y) - \frac{\alpha}{\gamma}$$
$$= \frac{c}{s}\left[\frac{(3\eta - 1 + \alpha y)}{(1-\eta)(1-\alpha y)} + \frac{(1-\alpha)y}{2\tilde{T}(1-\alpha y)^2\tilde{\omega}^2}\left\{2b - \frac{3a}{\tilde{\omega}^2} + 4\alpha y\left(\frac{a}{\tilde{\omega}^2} - b\right)\right\}\right] \quad (6)$$

The characteristic scaling parameters of pressure, volume and temperature, denoted by p^*, V^* and T^*, are combinations of the inter-segmental attraction energy ε^* and the segmental repulsion volume v^* for a segment of mass M_s, and again with $3c$ representing the number of external or volume-dependent modes in the s-mer. The importance of the c parameter was first recognized by Prigogine, Trappeniers and Mathot [22]. The scaling parameters are defined by the following relations

$$p^* = z(1-\alpha)\varepsilon^*/v^* \qquad V^* = sv^* \qquad T^* = z(1-\alpha)\varepsilon^*/(c_s R) \quad (7)$$

A comparison between theory and experimental equation-of-state data

serves to estimate the scaling parameters (p^*, T^*, V^*) or alternatively the molecular parameters (ε^*, v^*, c_s). The theory quantiatively describes the pvT data for solvents and polymers, including engineering plastics and their mixtures, at densities typical of the liquid state at low and high pressures [17, 22, 23].

In the further application of the theory to the glassy state, one needs to consider the fluctuations in free volume δh_{eq} which can be computed from [24–28]

$$\langle(\delta h_{eq})^2\rangle = \langle(h - \langle h\rangle_{eq})^2\rangle = kT\left(\left(\frac{\partial^2 A}{\partial y^2}\right)_{N,T,V}\right)^{-1} \tag{8}$$

NON-EQUILIBRIUM THEORY: GLASSY STATE AND GLASS TRANSITION

The dynamics of relaxation phenomena; stochastic theory

In contrast to polymer liquids, the same limited set of macroscopic variables does not suffice to fix the thermodynamic state of polymer glasses. Instead, the formation history of the glass influences the equation of state and other properties. It may be clear that the unambiguously defined melt state can serve as a good starting point for the simulation of glasses. A stochastic theory has been developed to describe the influence of formation history on the equation of state of polymer glasses and on the glass transition temperature. The theory is based on the RSC theory [24]. The assumption of a spatial distribution of free volume and, hence, mobility in the polymer system is made. Because the equilibrium is chosen as a reference state, this allows one to define both the free volume (distribution) and the mobility in a well-defined way. The free volume is identified with the order parameter h in the Holey–Huggins theory. The response of the system to a change in pressure and/or temperature is formed by a change in the actual free volume distribution to the new equilibrium.

It is assumed that the relaxation behaviour governing the glass transition region can be described by the approach to equilibrium of the conformational degree of freedom of the polymer backbone. Vibrational and side-group rotational degrees of freedom are assumed to be sufficiently fast and thus to respond almost instantaneously to variations in thermodynamic variables.

Consider now a change in temperature and/or pressure in the system from an initial to a final state. The thermodynamic properties change accordingly. It is our aim to monitor the kinetics of the changes. On a microscopic level, this change in macroscopic properties is caused by rearrangements in the polymer chains. A discussion of the interrelation between microscopic and macroscopic changes has been given in the context of the relaxation behaviour in polymer glasses [29]. The importance of the segmental rearrangements in the isolated chain and the influence of

the surrounding segments in the dense disordered state have been explained. Furthermore, the rate of change in the small volume element, containing the rearranging segments, is not only determined by the local segmental mobility but also by the possibility of the environment to assimilate the necessary changes.

However, our main interest is the kinetics of macroscopic properties and it is hoped that less detailed information concerning the microscopic state of the system should suffice to discuss these relaxation phenomena. It was suggested by Robertson [29] that the local free volume is an appropriate parameter with which to describe the local segmental mobility and, thus, the rate of rearrangements. The system is thought to be subdivided into small volume elements, each with its (local) free volume. The sample is thus characterized by a (time-dependent) free volume distribution. For mathematical convenience, it is assumed that this distribution is a set of n discrete levels $\{w_i(t), i = 1, n\}$. Changes in the occupation of the levels occur by transitions between the different levels and can be regarded as a stochastic process known as a Markov chain. The calculation of the evolution of the occupation of the free volume levels can be expressed in matrix form with the use of a transition probability matrix $\boldsymbol{P}(t)$. The time derivative of $\boldsymbol{P}(t)$ can be evaluated by the Chapman–Kolmogorov equation. A set of coupled differential equations ensues

$$\dot{\boldsymbol{P}}(t) = \boldsymbol{P}(t) \cdot \boldsymbol{A} \tag{9}$$

with $\boldsymbol{A}$ the generator matrix. In an infinitesimal time interval ($s \rightarrow 0$), only transitions between adjacent levels can occur. Then $\boldsymbol{A}$ becomes tridiagonal

$$\boldsymbol{A} = \begin{bmatrix} -\lambda_{1,2} & \lambda_{1,2} & 0 & . & . & . & 0 \\ \lambda_{2,1} & -\lambda_{2,1}-\lambda_{2,3} & \lambda_{2,3} & 0 & . & . & . \\ 0 & \lambda_{3,2} & -\lambda_{3,2}-\lambda_{3,4} & \lambda_{3,4} & 0 & . & 0 \\ . & . & . & . & . & . & \lambda_{n-1,n} \\ 0 & . & . & . & 0 & \lambda_{n,n-1} & -\lambda_{n,n-1} \end{bmatrix} \tag{10}$$

where $\lambda_{i,j}$ is the transition rate from state i to state j.

The formal solution of eqn. (9) is given by

$$\boldsymbol{P}(t) = \boldsymbol{P}(0)\, e^{\boldsymbol{A}t} \tag{11}$$

where $\boldsymbol{P}(0)$ is the initial transition probability matrix, in all applications set equal to the identity matrix $\boldsymbol{I}$. Equation (11) is solved by an eigenvalue analysis [30]. It can be shown that at sufficiently long times, the Markov chain $w(t)$ evolves to a stationary distribution $\{\xi_i, i = 1,n\}$

$$\lim_{t\to\infty} w(t) = [\xi_1 \quad . \quad \xi_i \quad . \quad \xi_n] \tag{12}$$

In this contribution, the stationary distribution is identified with the structure function h and its distribution defined in the HH theory [17, 27, 28]. For sufficiently small fluctuations, it can be shown that the fluctuations have a Gaussian distribution fully determined by $\langle h \rangle_{eq}$ and $\langle (\delta h_{eq})^2 \rangle$.

Transition rates: kinetics

In order to use the stochastic theory, the upward and downward transition rates $\lambda_{i,i+1}$ and $\lambda_{i+1,i}$, $1 \leq i \leq (n-1)$, respectively, must be defined. The functional dependence of the local transition rates on the regional free volume h_i is assumed to be identical with the dependence of the global mobility μ on the equilibrium overall free volume $\langle h \rangle_{eq}$. The global mobility of a system with free volume h can be defined, for example by a Williams–Landel–Ferry (WLF) type of equation [31]. On a local level, then, the mobility can be defined as

$$\mu_i \equiv \frac{b}{h_i - a} \tag{13}$$

For the local transition rates, the following expressions are used [24–30]

$$\lambda_{i,i-1} = \frac{R}{\beta^2} 10^{\mu_i} \sqrt{\frac{\xi_{i-1}}{\xi_i}}$$
$$\lambda_{i,i+1} = \frac{R}{\beta^2} 10^{\mu_i} \sqrt{\frac{\xi_{i+1}}{\xi_i}} \tag{14}$$

where R (in s^{-1}) contains a characteristic rate and a compensation for differences in global and local mobilities, β equals the difference in free volume content between two adjacent states, and the ratio of ξ values ensues from the balance equation.

The stochastic simulation

The numerical simulation procedure will be illustrated for a cooling experiment. A polymer melt, initially, at time t, temperature T and pressure p, is cooled isobarically at a rate T' (in $K\,s^{-1}$). At a certain temperature, the glass transition temperature will be reached and upon further cooling a polymer glass is formed. The stochastic simulation of the evolution of the free volume distribution with initial average $\langle h \rangle_{eq}$ and width $\langle (\delta h_{eq})^2 \rangle$ in this real time experiment proceeds along the following scheme [28]

1. Calculate the equilibrium properties (v, $\langle h \rangle_{eq}$, $\langle (\delta h_{eq})^2 \rangle$) at T and p corresponding to a time $t + \Delta t$.
2. Calculate the equilibrium distribution $\{\xi_i, i = 1,n\}$ at $t + \Delta t$.
3. Compute the transition rates using the equilibrium distribution and the actual distribution $\{w_i(t), i = 1,n\}$ at time t (eqns. (13) and (14)).
4. Determine the transition probabilities $\boldsymbol{P}(t)$ (eqns. (10) and (11)).
5. Update the actual distribution $\{w_i(t + \Delta t), i = 1,n\}$ at time $t + \Delta t$, using $\boldsymbol{P}(t)$.
6. Increment the time with Δt, and repeat steps 1–6.

A similar experiment can be done by, for example, specifying a pressurizing rate p' or by a simultaneous change in T and p. Furthermore,

T' and p' can be changed at will during the simulation. For example, at a given T and p in the glassy state, one can set $T' = 0$ and $p' = 0$ and from that time on monitor the physical ageing. It is thus possible to simulate the complete formation history of a polymer glass and to study the influence of these parameters on the resulting thermal properties.

During the simulation, the actual distribution $w(t)$ and the calculated average free volume $\langle h(t)\rangle_{ac}$ can differ from the equilibrium values. At sufficiently high temperatures, the actual and equilibrium values (and, of course, also the complete distributions) coincide; thus the system is equilibrated. At a certain temperature, the actual distribution $w(t)$ and also the actual average free volume $\langle h(t)\rangle_{ac}$ being to deviate from the equilibrium condition. Upon further cooling, the difference between actual and equilibrium states increases. As depicted in, for example Fig. 11, a transition temperature T_i can be obtained as the intercept of the extrapolated 'glassy' part of the curve with the equilibrium line. This transition temperature is now identified with the glass transition temperature T_g in the real experiment. Furthermore, the p, h, T data obtained from a specific simulation experiment can be used to compute the thermodynamic properties [28].

APPLICATIONS

Equilibrium equation of state of amorphous polymers

An illustration of the quality of the fit obtained with the equilibrium hole theory is given in Fig. 7 for the equation-of-state data for PS investigated

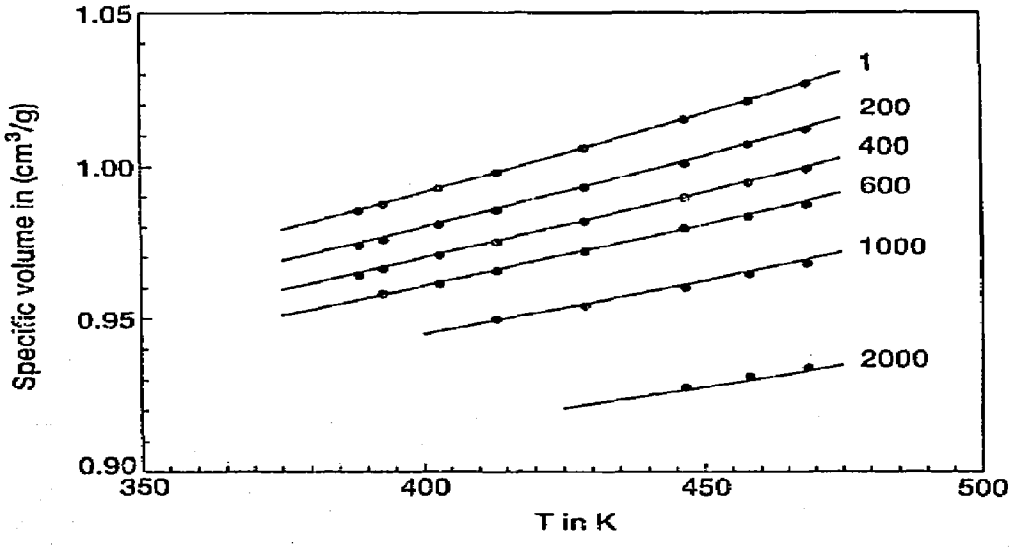

Fig. 7. Equation-of-state data for atactic polystyrene in the melt [2]. Lines are drawn according to the hole theory.

TABLE 1

Molecular characteristic parameters for some constituents

Polymer	p^*/MPa	v^*/cm^3 g^{-1}	T^*/K
Atactic polystyrene	679.7	0.9468	9438
Polyvinylacetate	895.5	0.8063	7988
Bisphenol-A polycarbonate	1000.5	0.7968	7929

over pressures up to 2 kbar [2]. The results displayed in Fig. 7 are typical for the many polymer systems investigated. The characteristic parameters for some constituents are summarized in Table 1. The predictions of the theory have also been examined for low molar mass compounds. Again, satisfactory comparisons have resulted for both homogeneous fluids and their mixtures [32]. Similar results have been obtained for polymer solutions and mixtures [33].

Non-equilibrium: the glassy state

Estimation of simulation parameters

The stochastic theory will be applied to the thermal behaviour of PVAc. With the scaling parameters (see Table 1), $\langle h \rangle_{eq}$ and $\langle (\delta h_{eq})^2 \rangle$ can be calculated. Subsequently, the full h distribution $\{\xi_i\}$ is calculated using a Gaussian approximation [28]. The parameters b and a in eqn. (13), describing the correlation between mobility and free volume, are obtained from experimental viscosimetric shift factors and are summarized in Table 2. The description of the shift factors with these parameters is shown in Fig. 8 by the line.

The parameter R (eqn. (14)) can be estimated from different kinds of experiments. In this application, following Robertson, Simha and Curro [24], we use the relaxation in a jump experiment [9] to obtain a value for R [27, 28]. The best description of this experiment (shown in Fig. 9) yields the value for the constant R given in Table 2. The set of parameters,

TABLE 2

Parameters for PVAc used in simulations

Parameter	Value	Parameter	Value
a (−)	0.392	R/s^{-1}	10^8
b (−)	0.0581		

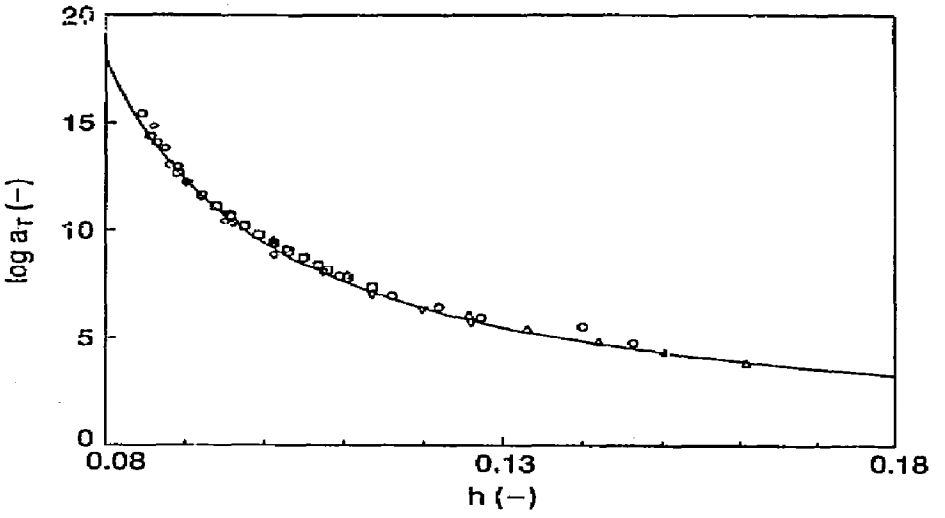

Fig. 8. Experimental dynamic mechanical shift factors versus the order parameter h for PVAc: □, dielectric [34]; ▽, dielectric [35]; ◇, creep; △, viscosity [36]; ○, stress relaxation [37]; —, fit of eqn. (13).

summarized in Table 2, is now fixed and we are ready to explore other dynamic simulations.

Simulation results: cooling rate and pressure

In Fig. 9, the computed volume relaxation behaviour brought about by single temperature jumps is compared to experimental [9] results [27, 28]. The observed agreement is typical for the present implementation of the stochastic theory as observed earlier [24]. The agreement can be improved by adopting a temperature-dependent R and more refined functions correlating the macroscopic mobility and free volume [24–26].

In Fig. 10, the simulated and experimental glass transition temperatures ar ambient pressure are presented as a function of cooling rate [27, 28]. In the simulations, the glass transition temperature is identified with the intercept of the extrapolated glass and liquid-like volume traces. An important observation is that the best R value derived from the jump experiment gives an accurate prediction of the glass transition temperature T_g at atmospheric pressure. This also suggests that the volumetric glass transition temperature, which is more commonly available than volume relaxation experiments, can be used to estimate the parameter R (eqn. (14)), which enables prediction of the volume relaxation behaviour for a given polymer under different conditions.

It is important to note that the sensitivity of volume relaxation experiments on R is significantly larger than that of predictions of T_g on R. Therefore, any reasonable value for R (even a 'universal' value, e.g.

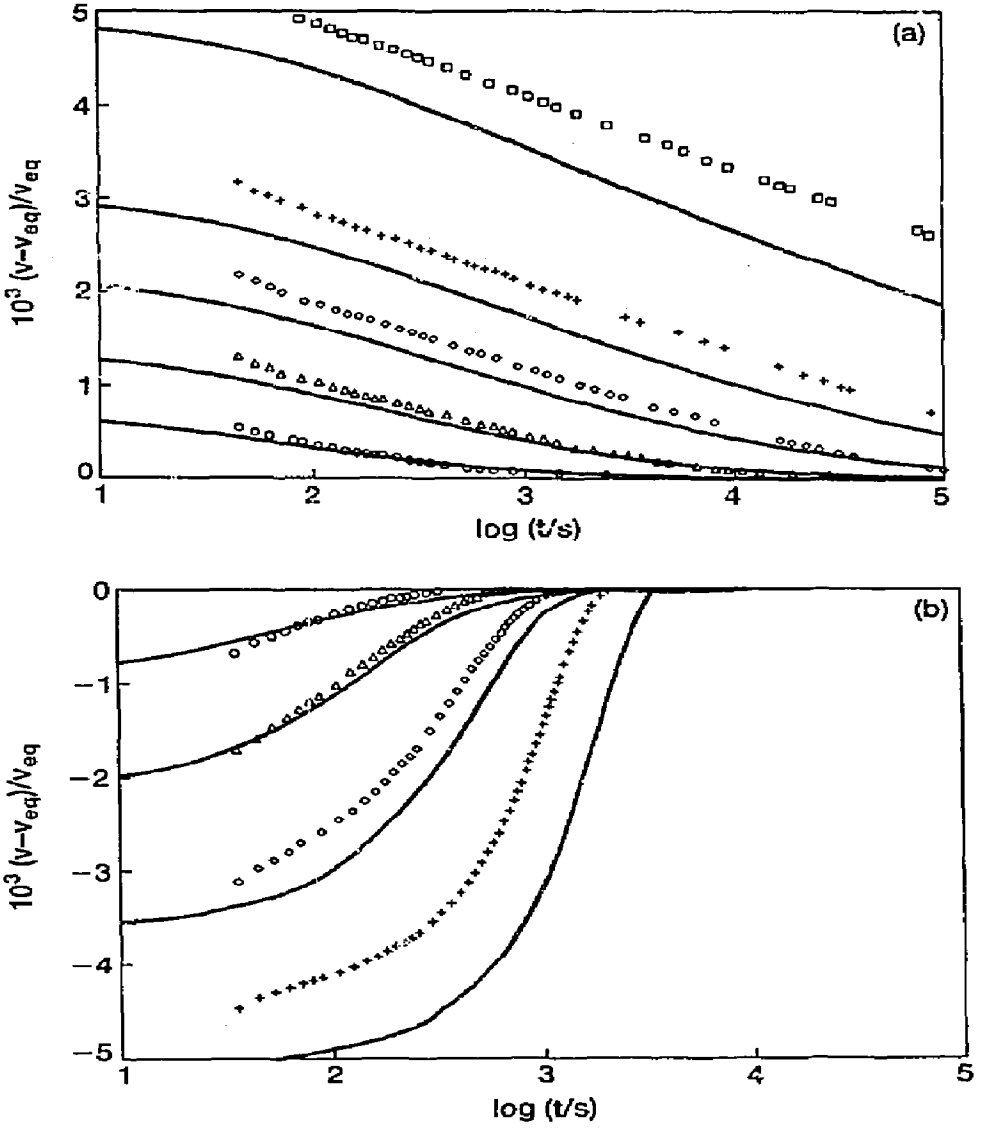

Fig. 9. Volume departure from equilibrium versus time after single temperature jumps for PVAc. Symbols, experimental data (Kovacs [9]). (a) Jumps from 40°C to: ○, 37.5°C; △, 35°C; ◇, 32.5°C; +, 30°C; and □, 25°C. (b) Jumps to 40°C from: ○, 37.5°C; △, 35°C; ◇, 32.5°C; and +, 30°C. Solid lines, calculated.

$R = 10^{10}$ [28]) will result in predictions of T_g that are at most only a few degrees off [38, 39].

The influence of pressure on the formation of the glassy state is shown in Fig. 11. The simulated formation conditions are chosen to mimic the experimental formation history (p and cooling rate T') [7]. The dependence of volume on temperature under isobaric cooling is depicted [28]. The agreement for the 0.1 MPa curve is excellent: maximum deviations between experimental and theoretical specific volumes Δv do not exceed

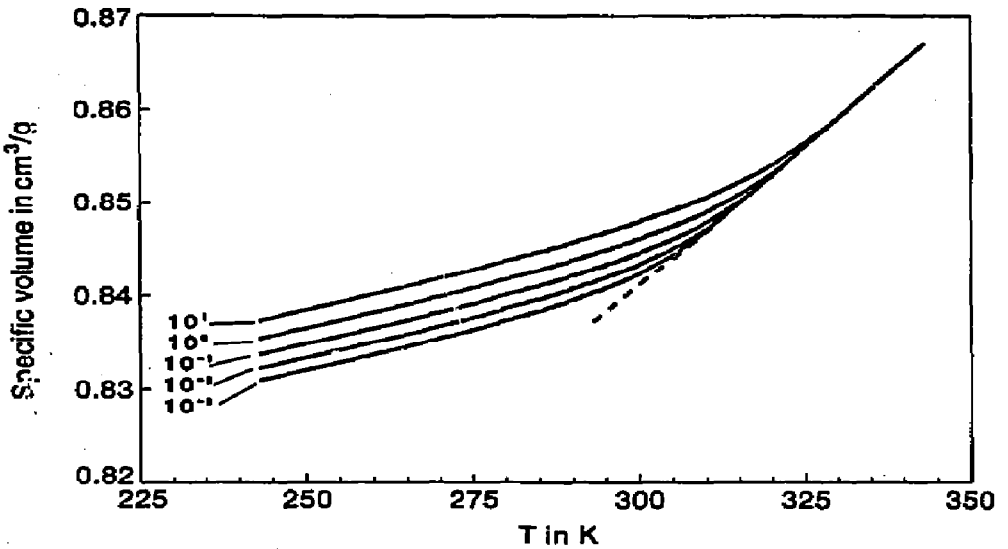

Fig. 10. Calculated specific volume versus temperature for the indicated cooling rates in K s $^{-1}$ for PVAc at ambient pressure. The broken line represents the equilibrium specific volume according to theory.

2×10^{-3} cm^3 g^{-1}. At higher pressures the predicted specific volumes are systematically too large but the maximum deviation Δv remains less than 8×10^{-3} cm^3 g^{-1} at $p = 80$ mPa. Values for the thermal expansion coefficient α_g and the glass transition temperature T_g extracted from the simulation relations compare favourably with experimental data. However, with

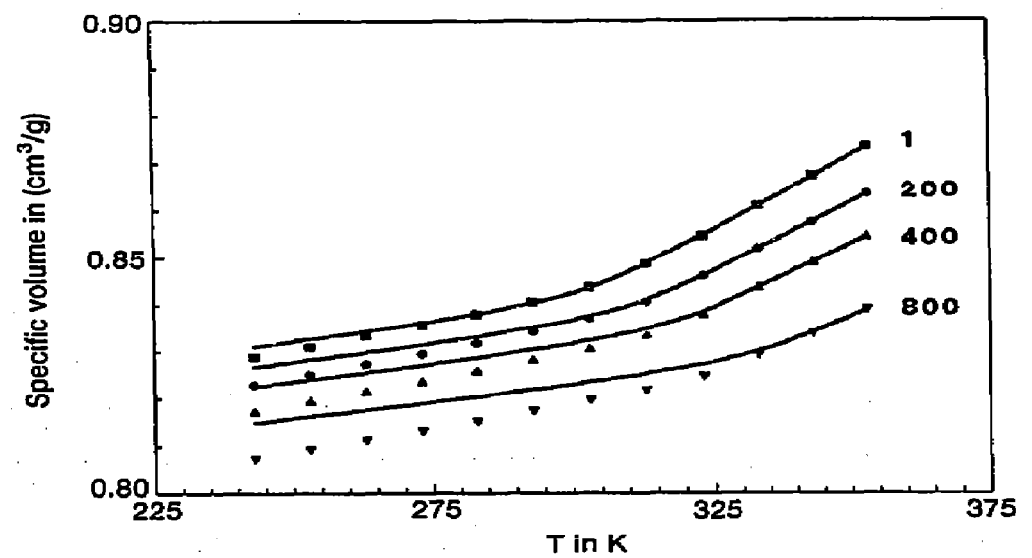

Fig. 11. Specific volume versus temperature for indicated formation pressures in bar for PVAc, cooled at 5 K h $^{-1}$. Solid lines, calculated isobars; symbols, experimental data, using a high-pressure mercury dilatometer [7].

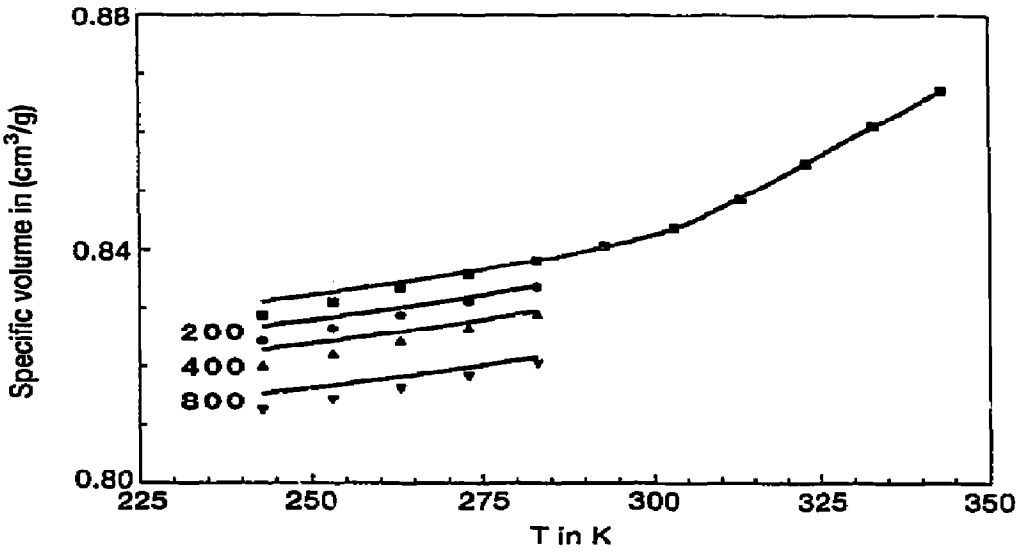

Fig. 12. Specific volume versus temperature for a PVAc glass formed by cooling at 5 K h^{-1} at 1 bar and subsequently pressurizing at approximately 400 bar h^{-1} to the indicated pressures in bar. Solid lines, calculated isobars; symbols, experimental data [7].

increasing pressure, systematic deviations occur between theory and experiment which can be attributed to too small a predicted value of the pressure dependence of the glass transition temperature (dT_g/dp) of PVAc glasses [28].

The simulated pvT behaviour of a polymer glass formed by cooling at 0.1 MPa and by subsequently pressurizing is shown in Fig. 12 together with experimental data [7]. Once more, the experimental formation history was reproduced accurately [28]. In this case the maximum deviation between experimental and theoretical volume Δv is smaller than 3×10^{-3} cm^3 g^{-1}. For a polymer glass formed by cooling a high-pressure polymer melt ($p = 80$ MPa) and by subsequently depressurizing, the results are depicted in Fig. 13, together with experimental data [7]. In this case, the deviations Δv are larger ($\Delta v < 8 \times 10^{-3}$ cm^3 g^{-1}) and can be mainly attributed to the overestimated pressure dependence of the glass transition temperature [28].

It has been shown [38, 39] that the inclusion of pressure data to define a relation between mobility and both pressure and temperature improves the prediction of the pressure dependence of T_g to an almost quantitative level.

For PVAc, results of the calculations are summarized in Table 3.

Dynamic compressibility

In previous applications [28, 39], experiments with a low characteristic rate were studied. We will now focus on experiments on a shorter time-scale, and investigate the influence of time and frequency on the response of a polymer system. This is shown from the simulation of the

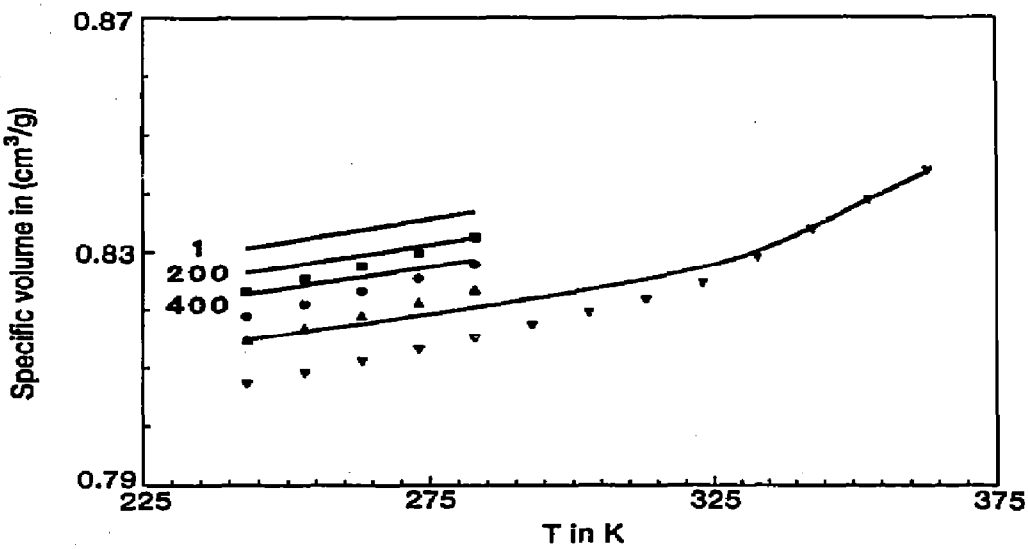

Fig. 13. Specific volume versus temperature for a PVAc glass formed by cooling at 5 K h^{-1} at 800 bar and subsequently depressurizing at approximately 400 bar h^{-1} to the indicated pressures in bar. Solid lines, calculated isobars; symbols, experimental data [7].

TABLE 3

Comparison of calculated quantities [27, 28] with experimental data [7, 40] for PVAc

Property	Exper.	Calc.	Formation history	
			p/MPa	q/K s^{-1}
T_g/K		314.5	0.1	10
		310.0	0.1	1
		306.2	0.1	0.1
		303.1	0.1	0.01
		300.7	0.1	0.001
dT_g/d(log cooling rate)/K	2.9[a]	3.5	0.1	0.001–10
T_g/K	304.7	301.0	0.1	0.00139
	309.7	307.3	20	0.00139
	314.2	314.0	40	0.00139
	321.6	327.1	80	0.00139
dT_g/dp/K MPa^{-1}	0.212	0.33	0.1–80	0.00139
α(0.1 MPa glass, 273 K)/K^{-1}	2.86×10^{-4}	2.24×10^{-4}	0.1	0.00139
	2.59×10^{-4}	2.03×10^{-4}	80	0.00139
β(0.1 MPa glass, 273 K)/MPa^{-1}	2.75×10^{-4}	2.64×10^{-4}	0.1	0.00139
	2.54×10^{-4}	2.32×10^{-4}	80	0.00139
α(80 mPa glass, 273 K)/K^{-1}	2.94×10^{-4}	1.96×10^{-4}	0.1	0.00139
	2.63×10^{-4}	1.74×10^{-4}	80	0.00139
β(80 MPa glass, 273 K)/MPa^{-1}	2.70×10^{-4}	2.65×10^{-4}	0.1	0.00139
	2.42×10^{-4}	2.31×10^{-4}	80	0.00139

[a] Based on enthalpic data in the range $0.005 \leq q \leq 0.17$ K s^{-1}.

dynamic compressibility of PVAc, for which experimental data are available [12]. To predict dynamic behaviour, no new parameters have to be introduced. Because we will only predict atmospheric pressure data, the issue of pressure dependence of mobility discussed earlier [39] is not relevant here.

In the simulations, a sinusoidal and isothermal pressure change with an amplitude of 0.2 MPa (this is well within the linear region) and a cycle frequency of ν Hz was used. After four cycles, a steady-state response was observed. From the phase shift between the sinusoidal pressure and the response of the system (the volume), an analysis can be made in terms of storage and loss components B' and B'', respectively, of the dynamic compressibility B. From B' and B'', $\tan\delta$ can also be calculated. In Fig. 14, the isothermal compressibility is plotted versus frequency for several temperatures. In the melt-like state, i.e. at low frequencies, the behaviour is completely viscous. The level of B' is here related to the equilibrium compressibility and shows a temperature dependence. In the glass-like state, i.e. at high frequencies, the behaviour is fully elastic. There B' is related to the compressibility of a glass, which hardly shows temperature dependence. It is clear that for each temperature, an increase in the frequency results in a transition from a melt-like (high B') to a glass-like (low B') behaviour, via a transition region where B'' and $\tan\delta$ reach a maximum. As is also found experimentally [41], the maximum in $\tan\delta$ is always located at higher frequencies, compared to the maximum in B''.

Enthalpy

The configurational part of the enthalpy h can be obtained from the HH theory [38]. With increasing pressure, the average segment distance decreases due to compressibility. While the system can be described with a Lennard-Jones potential, this will result in a less favourable situation when the sum of all intermolecular contacts is considered. In Fig. 15 the calculated enthalpy is plotted for PVAc glasses formed at different pressures [28, 38, 39]. The volume of these glasses has already been presented in Fig. 11. The predicted enthalpy data can be compared to experimental data. As an example, at 30°C and 0.1 MPa, simulations yield $\Delta h = h_{net} - h_{eq} = 0.7\ \mathrm{J\,g^{-1}}$ for a cooling rate of $5\ \mathrm{K\,h^{-1}}$, and $\Delta h = 1.5\ \mathrm{J\,g^{-1}}$ for a cooling rate of $1\ \mathrm{K\,s^{-1}}$. Experimental data by Cowie et al. [42] show an initial Δh at 30°C of $1.9\ \mathrm{J\,g^{-1}}$ for a quenched ($40\ \mathrm{K\,min^{-1}}$) PVAc glass. Experimental data on a PVAc glass cooled at $0.31\ \mathrm{K\,min^{-1}}$ reported by Sasabe and Moynihan [40] yield $\Delta c_p = c_{p,l} - c_{p,g} = 0.5\ \mathrm{J\,g^{-1}\,K^{-1}}$ at 30°C. For the same cooling rate, calculations yield $\Delta c_p = 0.32\ \mathrm{J\,g^{-1}\,K^{-1}}$. If the derivative of enthalpy with respect to time is monitored during cooling and heating runs, differential scanning calorimetry (DSC) experiments are simulated. As an illustration, in Fig. 16 some simulations of DSC experiments on PS are compared to experimental data [43] for identical thermal history. The

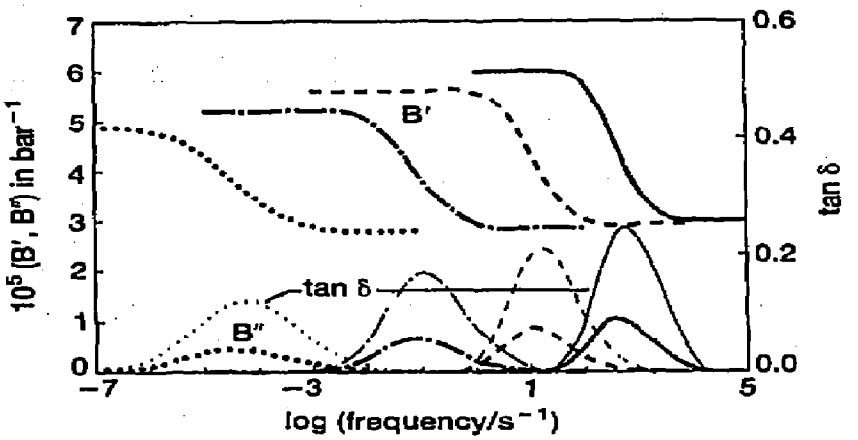

Fig. 14. Calculated equilibrium dynamic compressibility versus frequency for PVAc at 1 bar. The storage compressibility B', the loss compressibility B'' and tan δ at: —, 75°C; – – –, 60°C; –·–·–, 45°C; · · ·, 30°C.

height of the normalized c_p peaks shows excellent agreement with experiments; the location is shifted to lower temperatures over about 8 K.

With these few examples it has been shown that the presented stochastic theory is capable of predicting energy-related properties, as well as the earlier presented [28, 38, 39] volume-related properties. Good qualitative agreement is obtained. No new parameters have to be introduced. The possibility to relate enthalpic, volumetric and mechanical properties not only during the process of glass formation but also during physical ageing might contribute to a further understanding of the relationships between these properties. Also, a theoretical analysis of glass formation in terms of the Ehrenfest relations is now possible. Evaluation of the Prigogine–Defay ratio has been published elsewhere [38].

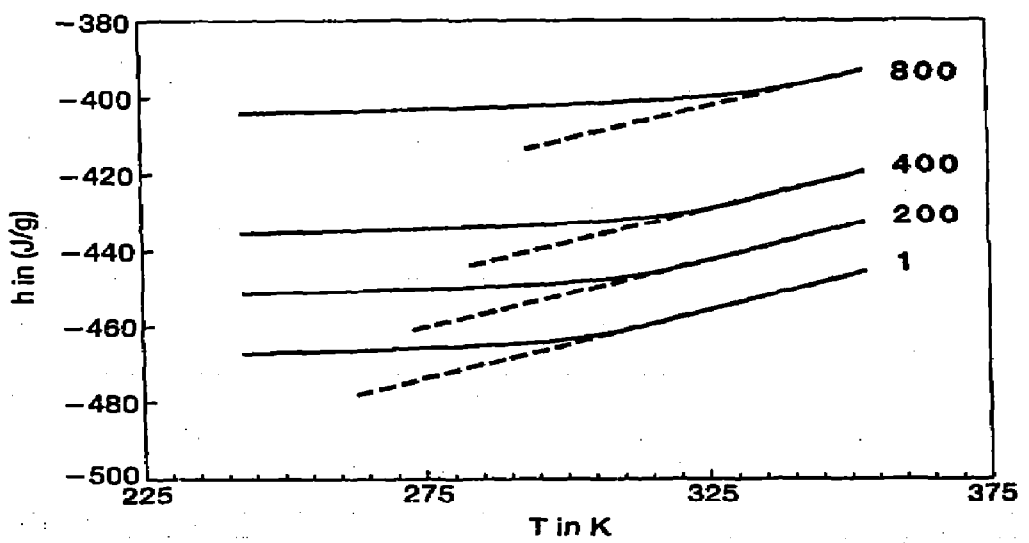

Fig. 15. Calculated specific enthalpy versus temperature for PVAc glasses cooled at 5 K h^{-1} at the indicated pressures in bar. Broken lines represent the equilibrium specific enthalpy.

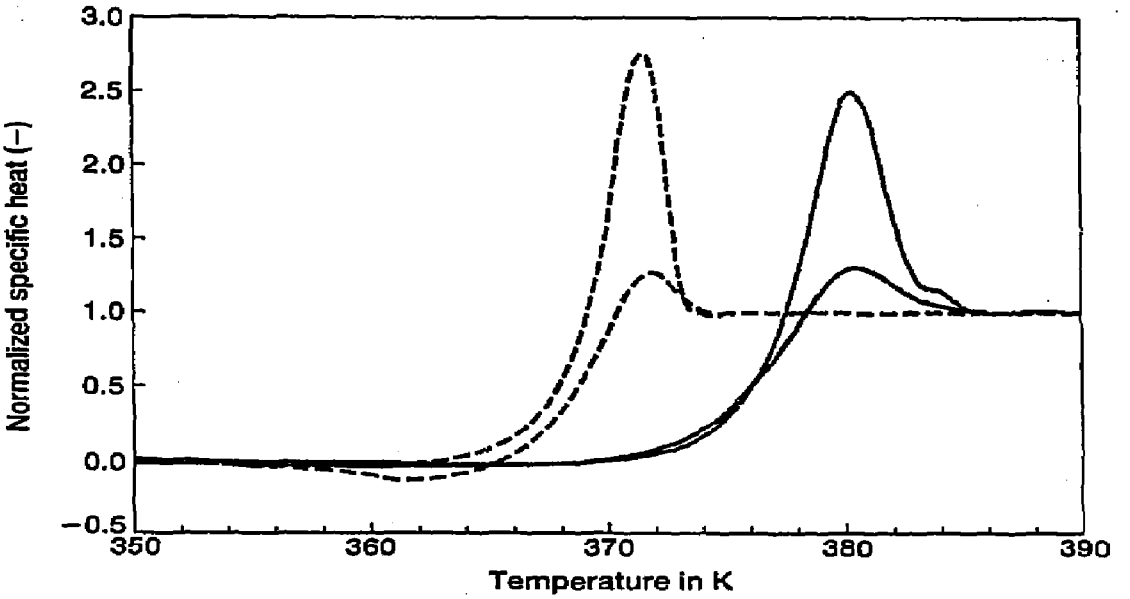

Fig. 16. The normalized specific heat $(c_p - c_{pg})/(c_{pe} - c_{pg})$ versus temperature for PS, with c_p, c_{pg} and c_{pe} the actual, glassy and equilibrium specific heat capacities, respectively. Values during heating at 10 K min^{-1} from 300 K after the following thermal history: cooling at 40 K min^{-1} from 420 K to a temperature T_a; ageing at T_a for a time t_a; cooling at 40 K min^{-1} from T_a to 300 K: – – –, simulations; —, experimental [8]. Upper curves, $t_a = 3600$ s; lower curves, $t_a = 0$ s.

Injection moulding

The presented stochastic formalism enables the calculation of the influence of formation history on several properties of the glass. In particular, the influence on volumetric properties has been discussed so far.

These calculations have been combined with simulations of injection moulding processes [44, 45]. In these simulations the glass formation plays an important role, while simultaneously molecular orientation and stresses in the final product have to be accounted for. The influence of the injection moulding history on the pvT behaviour of the glass can be evaluated with the presented theory. This can be done separately at several locations in the mould, where different pressure–temperature–time paths have been followed. These calculations can be performed for amorphous polymers in general, with the use of parameters determined in the polymer melt (Tables 1 and 2). Further implications of, for example, physical ageing for the detailed density profile are still under investigation.

CONCLUSIONS

The combination of pressure and temperature results in a much more extensive dependence of many physical properties than the varation of, for example, temperature alone. In the case of single constituents, the influence

of pressure has been examined. Finally, the influence of pressure on the glass transition temperature and the glassy state itself was discussed. In particular, the importance of the formation route and the occurrence of volume relaxation was demonstrated. The molecular mechanism responsible for the glass transition leads to the study of the time dependence or high-frequency behaviour of thermodynamic properties.

The equilibrium theory outlined yields quantitatively successful equations of state for dense disordered assemblies of low and high molar mass constituents, and their mixtures. With a limited set of parameters, a quantitative description of pvT data is obtained at densities typical of the liquid state at ambient and elevated pressures. This excellent description of the equation-of-state data also contributes to the accurate prediction of, for example, the complicated influence of pressure found in miscibility behaviour [18].

The presented stochastic theory offers a route to extend the description and prediction of equation-of-state data through the glass transition region into the glassy state. The equation-of-state behaviour of glasses, the glass transition temperature and its dependence on formation history are predicted from equilibrium pvT data, equilibrium dynamic mechanical shift factors and a single non-equilibrium volume relaxation experiment. Simulations at ambient pressure show excellent agreement with experimental data. Discrepancies between theory and experiment at high pressures are almost entirely related to the dependence of T_g on the glass formation pressure [28, 38, 39]. The use of shift factor data, obtained at ambient pressure, to obtain a relation between mobility and free volume, is probably limited to low pressures. Discrepancies at high pressures, as shown in this contribution, suggest that mobility at high pressure is not described by the order parameter h alone, which is here used as a measure for free volume. It has been shown [38, 39] that the inclusion of pressure data to define a relation between mobility and both pressure and temperature improves the prediction of the influence of pressure on T_g.

The only non-equilibrium data used for the predictions are volume data of a single relaxation experiment, to estimate a value for R. As is shown in this contribution, the parameter R can also be estimated from different experiments, e.g. the location of the ambient glass transition temperature. Also other properties, e.g. dynamic compressibility, enthalpy relaxation, dynamic light scattering, are being simulated and investigated for PVAc and other polymers as well, e.g. polycarbonate, polystyrene, polymethylmethacrylate [38, 39].

REFERENCES

1 P. Zoller, in J. Brandrup and E.H. Immergut (Eds.), Polymer Handbook, John Wiley, New York, 1989, p. VI/475.
2 A. Quach and R. Simha, J. Appl. Phys., 42 (1971) 4592.

3 R.A. Haldon and R. Simha, Macromolecules, 1 (1968) 340.
4 R. Greiner and F.R. Schwarzl, Rheol. Acta, 23 (1984) 378.
5 R. Simha, Macromolecules, 10 (1977) 905.
6 R.N. Haward, The Physics of Glassy Polymers, Appl. Sci. Publ., London, 1973.
7 J.E. McKinney and M. Goldstein, J. Res. Nat. Bur. Stand. Sect. A Phys. Chem., 78 (1974) 331.
8 G.J. Kogowski and F.E. Filisko, Macromolecules, 19 (1986) 828.
9 A.J. Kovacs, Fortschr. Hochpolym. Forsch., 3 (1963) 394.
10 G. Goldbach and G. Rehage, Rheol. Acta, 6 (1967) 30.
11 G. Goldbach and G. Rehage, J. Polym. Sci. Part C, 16 (1967) 2289.
12 J.E. McKinney and H.V. Belcher, J. Res. Nat. Bur. Stand. Sect. A, 67 (1963) 43.
13 G.D. Patterson, J.R. Stevens and P.J. Carrol, J. Chem. Phys., 77 (1982) 622
14 J.J. Tribone, A.M. Jamieson and R. Simha, J. Polym. Sci., Polym. Symp., 71 (1984) 231.
15 G. Fytas, Macromolecules, 22 (1989) 211.
16 R. Simha and T. Somcynsky, Macromolecules, 2 (1969) 341.
17 E. Nies and A. Stroeks, Macromolecules, 23 (1990) 4088.
18 A. Stroeks and E. Nies, Macromolecules, 23 (1990) 4092.
19 E. Nies and H. Xie, Macromolecules, 26 (1993) 1683.
20 H. Xie and E. Nies, Macromolecules, 26 (1993) 1689.
21 E. Nies and H. Xie, Makromol. Chem., Macromol. Symp., 58 (1992) 227.
22 I. Prigogine, N. Trappeniers and V. Mathot, Discuss. Faraday Soc., 15 (1953) 93.
23 R.K. Jain and R. Simha, J. Chem. Phys., 72 (1980) 4909.
24 R.E. Robertson, R. Simha and J.G. Curro, Macromolecules, 17 (1984) 911.
25 R.E. Robertson, R. Simha and J.G. Curro, Macromolecules, 18 (1985) 2239.
26 R.E. Robertson, R. Simha and J.G. Curro, Macromolecules, 21 (1988) 3216.
27 S. Vleeshouwers and E. Nies, Polymer Commun., 32 (1991) 418.
28 S. Vleeshouwers and E. Nies, Macromolecules, 25 (1992) 6921.
29 R.E. Robertson, J. Polym. Sci., Polym. Phys., 17 (1979) 597.
30 R. Goodman, Introduction to Stochastic Models, Benjamin/Cummings, Menlo Park, California, USA, 1988, p. 127.
31 M.I. Williams, R.F. Landel and J.D. Ferry, J. Am. Chem. Soc., 77 (1955) 3701.
32 R.K. Jain and R. Simha, Macromolecules, 13 (1980) 1501.
33 R. Simha and R.K. Jain, J. Colloid Polym. Sci., 263 (1985) 905.
34 M.L. Williams and J.D. Ferry, J. Colloid Sci., 9 (1954) 479.
35 J.M. O'Reilly, J. Polym. Sci., 57 (1962) 429.
36 D.J. Plazek, Polym. J. (Tokyo), 12 (1980) 43.
37 K. Ninomiya and H. Fujita, J. Colloid Sci., 12 (1957) 204.
38 S. Vleeshouwers, Modelling and Predicting Properties of Polymers in the Amorphous Glassy State, Dissertation, Eindhoven University, The Netherlands, 1993.
39 S. Vleeshouwers and E. Nies, submitted.
40 H. Sasabe and C.T. Moynihan, J. Polym. Sci. Polym. Phys. Ed., 16 (1978) 1447.
41 J.D. Ferry, Viscoelastic Properties of Polymers, Wiley, New York, 1980.
42 J.M.G. Cowie, S. Elliot, R. Ferguson and R. Simha, Polym. Commun., 28 (1987) 298.
43 I.M. Hodge and G.S. Huvard, Macromolecules, 16 (1983) 371.
44 G.G.J. Schennink, On the Dimensional Stability of Injection Moulded, Amorphous Thermoplastic Products, Report, Eindhoven University, The Netherlands, 1993.
45 L.W. Caspers and G.G.J. Schennink, Numerical Simulation of the Physical Ageing of Injection Moulded Products, Abstract, 8th Annual Meeting of Polym. Proc. Soc., New Delhi, Polym. Proc. Soc., New Dehli, India, 1992.